CHEMICAL ENGINEERING TRANSACTIONS
VOL. 109, 2024
A publication of AIDIC
The Italian Association of Chemical Engineering
Online at www.cetjournal.it
Guest Editors: Leonardo Tognotti, Rubens Maciel Filho, Viatcheslav Kafarov

ISBN 979-12-81206-09-0; **ISSN** 2283-9216
DOI: 10.3303/CET24109023

Catalytic Conversion of 1,2-propanediol to 2-propanone: An Exploratory Study

Alejandro Lete, Lucía García*, Joaquín Ruiz, Jesús Arauzo

Thermochemical Processes Group (GPT) Aragon Institute of Engineering Research (I3A), Universidad de Zaragoza, Mariano Esquillor S/N, 50018, Zaragoza, Spain
luciag@unizar.es

Climate change underscores the urgency of exploring novel pathways for the decarbonization of the transportation sector. Within the aviation sector, biofuel appears to be the most viable short-term solution. Recently, the focus has centered on the aldol condensation of biomass-derived furans with ketones as 2-propanone (acetone) or 2-hydroxy-2-propanone (acetol), offering an efficient method to produce intermediates suitable for aviation fuels. However, 2-propanone is currently produced from cumene, a petroleum-derived source. This study proposes 1,2-propanediol (1,2-PDO), a sustainable product obtained by the hydrogenolysis of glycerol, a byproduct of the biodiesel industry, as a renewable feedstock for the generation of 2-propanone. For that purpose, the coprecipitation method with sodium hydroxide was employed to synthesize three copper, zinc, and aluminum-based catalysts. The catalysts were characterized through ICP-OES, N_2 adsorption-desorption, XRD, and H_2-TPR. The dehydration of 1,2-PDO to 2-propanone was investigated in a continuous system at 227 ºC, using a 10 wt% aqueous solution of 1,2-PDO at atmospheric pressure with a W/m ratio of 10 $g_{Catalyst}$ min $g_{1,2\text{-PDO}}^{-1}$. The catalyst with the lower zinc content achieved the highest carbon selectivity to 2-propanone at 22.1% and generated 1845 $\mu mol_{2\text{-propanone}}/mol_{1,2\text{-PDO}}$. This study revealed that lower zinc content could enhance 1,2-PDO dehydration to 2-propanone, preventing the subsequent hydrogenation of 2-propanone to 2-propanol. Additional optimization is required to attain higher yields.

1. Introduction

The persistent use of petroleum has caused severe environmental issues with potentially fatal consequences, primarily due to the ongoing emission of greenhouse gases. It is estimated that its usage will continue to rise from 15.4 billion liters per day in 2018 to 17.8 billion liters per day by 2035 (Li et al., 2020). In particular, the transportation sector stands out as one of the most dependent, and exploring alternatives to fossil fuels is a matter of great global interest that could contribute to mitigating the effects of climate change. Currently, several alternatives in transportation utilize renewable energy, such as biofuels, and electric or hydrogen-powered vehicles. However, in the aviation sector, the only successfully implemented renewable option has been biofuels, using organic compounds derived from biomass. There are up to four technologies for generating biofuels suitable for aviation (Oil to jet fuels (OTJ), Gas to jet fuels (GTJ), Alcohol to jet fuels (ATJ), and Sugars to jet fuels (STJ)). Still, two of these technologies (OTJ and GTJ) are not able to produce all the necessary types of hydrocarbons for optimal combustion and need to be blended with fossil fuel (Khan et al., 2019). To address this issue, the focus has shifted to the STJ route. This technology has a middle step, known as aldol condensation, which involves the union of furans derived from biomass as furfural with ketones such as 2-propanone (acetone) or 2-hydroxy-2-propanone (acetol), achieving conversions of over 95 % (West et al., 2008). The resulting products are aviation intermediates that would enable the subsequent generation of all required types of hydrocarbons through a hydrogenation stage, allowing for the full utilization of biofuels in aviation (Yang et al., 2018). Conversely, the STJ process is not entirely renewable because up to 95% of global 2-propanone is derived from petroleum through phenol production, and acetol is generated from bromoacetone, potassium formate, or 2-propanone (Basu and Sen, 2021).

Paper Received: 1 December 2023; Revised: 26 February 2024; Accepted: 23 March 2024
Please cite this article as: Lete A., García L., Ruiz J., Arauzo J., 2024, Catalytic Conversion of 1,2-propanediol to 2-propanone: an Exploratory Study, Chemical Engineering Transactions, 109, 133-138 DOI:10.3303/CET24109023

The main solution could come from glycerol, the major byproduct of biodiesel manufacturing. Global biodiesel production is on the rise, and it has led to a global oversupply of glycerol, lowering its cost, and it is expected to have stable availability in the future (Checa et al., 2020). These circumstances have turned glycerol into a key platform for new routes of sustainable and cost-effective chemical production, enabling the profitability and enhancement of the biodiesel industry. One of the most extensively studied reactions involving glycerol is hydrogenolysis, with its primary product being 1,2-propanediol (1,2-PDO), a crucial commodity chemical with diverse applications that is employed as a precursor to various products such as propanal, 1-propanol, 2-propanol, or 2-propanone (Restrepo et al., 2021). The dehydration reaction of 1,2-PDO produces propanal and 2-propanone but across all the literature articles, the generated amount of 2-propanone has been residual in all cases (Courtney et al., 2012). This suggests that the studied dehydration of 1,2-PDO over catalysts based on tungsten, vanadium, and chromium, along with the operating conditions, have not been optimal for its production (Mori et al., 2009). Under this premise, this study is focused on the potential pathway of 1,2-PDO to 2-propanone using catalysts based on copper, zinc, and aluminum. This research serves as an initial exploration into the feasibility of obtaining 2-propanone from a renewable source, addressing a gap in the existing studies.

2. Experimental

2.1 Catalyst preparation

Three catalysts were synthesized by employing the coprecipitation method described by Inui et al. (2002), using a constant amount of copper while varying the amount of zinc and aluminum. The molar ratios employed were Cu:Zn:Al = 2:4:1, 2:3:2, and 2:2:3, and the resulting catalysts were named CZAN-1, CZAN-2, and CZAN-3 respectively. The corresponding amount of metallic nitrates of copper, zinc, and aluminum were dissolved in milli-Q water at 40 °C and a 3 M solution of sodium hydroxide was used as precipitant. After precipitation, each precipitate was washed, filtered, and dried at 105 °C for 16 hours. The catalysts were then calcined at 675 °C for 3 hours and sieved to a particle size of 160 – 315 µm.

2.2 Catalyst characterization

The textural and physicochemical properties of the catalysts were analyzed using four different techniques. Chemical composition was determined by inductively coupled plasma optical emission spectrometry (ICP-OES) with a Thermo Elemental ISIS Intrepid Radial instrument equipped with a Timberline IIS automatic injector. The textural properties of the fresh catalysts were analyzed by N_2 adsorption-desorption with an Autosorb iQ3 from Quantachrome Instrument and the crystalline phases in the catalysts were determined through X-ray diffraction using a D-Max Rigu 300 diffractometer with a rotating copper anode and a graphite monochromator. The reducibility of the catalysts was analyzed by programmed temperature reduction (H_2-TPR) with Micromeritics AutoChem II 2920 equipment. More information about the conditions used in the analyses can be found in Raso et al. (2023).

2.3 Installation and operating conditions

The experiments were conducted using a small laboratory-scale system developed by PID (Process Integral Development Eng & Tech, Spain). Key components of the facility include a tubular quartz reactor (9 mm of internal diameter), a high-performance liquid chromatography (HPLC) pump, mass flow controllers, and a condensation system located at the reactor outlet for the collection of liquids. The catalysts were tested for 2 hours at 227 ºC, under atmospheric pressure, with a catalyst mass of 0.1 g. The catalyst was mixed with 0.13 g of sand of the same particle size to ensure isothermicity in the catalytic bed. Prior to the reaction, the catalysts were activated, using a H_2 flow of 100 cm^3 STP/min. The feed employed was a 10 wt% aqueous 1,2-PDO solution that was introduced into the reactor with a flow rate of 0.1 mL/min. The product gases were analyzed online using an Agilent 490 Micro-GC gas chromatograph coupled with Thermal Conductivity Detectors (TCD), employing an N_2 flow rate of 40 cm^3 STP/min as an internal standard. The liquid products were condensed and analyzed offline with an Agilent 7890 GC gas chromatograph equipped with a Flame Ionization Detector (FID) and an HP-FFAP Agilent 19091F-105 capillary column, with 1-butanol serving as the internal standard.

2.4 Catalytic performance evaluation

The experimental results were analyzed to study the selective dehydration of 1,2-PDO to 2-propanone. To this end, three parameters were defined to compare the catalytic activity of the CZAN catalysts. Carbon yield to gaseous and liquid products (Eq(1) and Eq(2) respectively) was defined as the ratio of the total carbon moles of each compound to the carbon moles fed to the system (n^0). The carbon selectivity to liquid products (Eq(3)) was defined as the carbon moles of a compound divided by the total carbon moles of the analyzed liquid products.

$$X_{Gas}\ (\%) = \frac{n_{CO_2}}{n^0} \cdot 100 \quad (1)$$

$$X_{Liq}\ (\%) = \frac{n_{MeOH} + 2 \cdot n_{EtOH} + 3 \cdot n_{2\text{-propanol}} + 3 \cdot n_{2\text{-propanone}} + 3 \cdot n_{Acetol} + 2 \cdot n_{Acetic\ Acid} + 2 \cdot n_{Acetaldehyde}}{n^0} \cdot 100 \quad (2)$$

$$S_i\ (\%) = \frac{\text{carbon number of compound } i \cdot n_i}{n_{MeOH} + 2 \cdot n_{EtOH} + 3 \cdot n_{2\text{-propanol}} + 3 \cdot n_{2\text{-propanone}} + 3 \cdot n_{Acetol} + 2 \cdot n_{Acetic\ Acid} + 2 \cdot n_{Acetaldehyde}} \cdot 100 \quad (3)$$

3. Results and discussion

3.1 Catalyst characterization

The chemical composition and textural properties of CZAN catalysts are shown in Table 1.

Table 1: Chemical composition and textural properties of the catalysts.

Catalyst	Cu (wt%)	Zn (wt%)	Al (wt%)	Na (wt%)	S_{BET} (m^2/g)	V_P (cm^3/g)	d_p (nm)	CuO (nm)	ZnO (nm)
CZAN-1	27.7	58.5	6.0	7.7	5.3	0.04	3.2	28.2	42.2
CZAN-2	28.9	45.9	12.5	12.7	5.2	0.04	3.2	25.2	38.3
CZAN-3	34.8	35.6	22.2	7.4	32.2	0.11	15.0	24.1	22.7

The target metal content of the catalysts was achieved, but some of the sodium used during coprecipitation has adhered to the catalyst. A study conducted by Kinage et al. (2010) concluded that the addition of 5 wt% of sodium in metal catalysts favors the dehydration reaction of glycerol to acetol, so it could help carry out dehydration from 1,2-PDO to 2-propanone. The N_2 adsorption-desorption isotherms showed that the CZAN-3 catalyst has a type IV(a) isotherm, according to the IUPAC classification, typical of mesoporous solids. In contrast, the CZAN-1 and CZAN-2 catalysts have type III adsorption isotherms, typical of macroporous or non-porous materials. The S_{BET} of the catalysts depends on the amount of aluminum, which acts as a support, and the CZAN-3 catalyst, with the highest amount of aluminum, shows the largest surface area (32.2 m^2/g). The catalysts CZAN-1 and CZAN-2 have similar properties, possibly because the catalyst CZAN-2 has a higher amount of sodium, and its surface area has been reduced (Kruissink et al., 1981). The d_p of the CZAN-3 catalyst (15 nm) stands out, which is almost five times higher than the rest of the catalysts.
The crystalline phases detected in the catalysts are shown in Figure 1 (A).

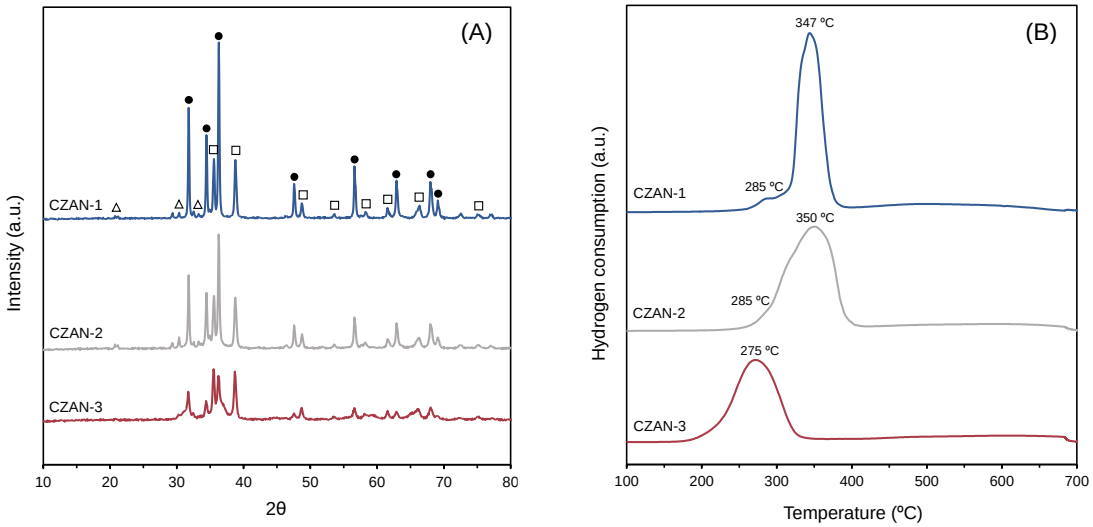

Figure 1: XRD patterns of the calcined CZAN catalysts. (Δ) *$NaAl_2O_4$;* (•) *ZnO;* (O) *CuO (A). TPR profiles of calcined CZAN catalysts (B).*

The catalysts are crystalline and show definite diffraction peaks. Zinc appeared in the form of zinc oxide (ZnO) (JCPDS 01-075-0576) with characteristic diffraction peaks at the 2θ positions of 31.7 °, 34.4 °, 36.3 °, 47.4 °, 56.7 °, 62.8 °, 68.0 ° and 69.0 °. Copper was incorporated in the form of copper oxide II (CuO) (JCPDS 01-072-0629) and its presence can be detected in its characteristic 2θ diffraction peaks of 35.3 º, 38.8 º, 48.5 º, 53.9 º, 58.6 º, 61.8 º, 66.6 º and 75.5 º. The sodium adhered during coprecipitation has formed $NaAlO_2$ (JCDPS 01-

083-0316) with its distinguishing diffraction peaks at 2θ of 20.8 º, 30.2 º and 33.6 º. The average crystallite sizes of the CuO and ZnO phases were calculated using the Scherrer equation from the diffraction peaks at 38.8 and 31.7 º respectively and are shown in Table 1. The amount of copper and zinc could affect the crystallite size. In the case of zinc, larger amounts have resulted in larger ZnO crystallites, while the opposite happened with copper. The surface morphology of the fresh catalysts was analyzed by microscopic photography (Figure 2). Catalysts with higher amounts of sodium tend to generate greater agglomeration of particles on the surface (Song et al., 2023). This fact can be observed in the CZAN-2 catalyst, with the highest amount of sodium (12.7 wt%), which shows a rugose surface with greater agglomeration.

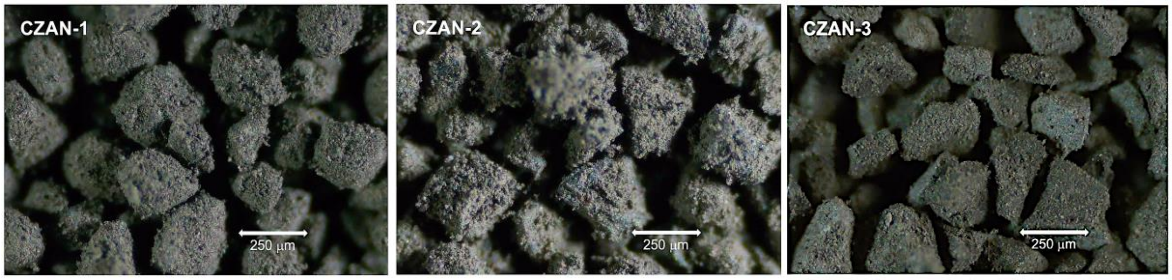

Figure 2: Microscope images of the fresh catalysts.

The TPR reduction profiles of the catalysts are shown in Figure 1 (B). The CZAN-3 catalyst shows a single reduction peak at 275 °C. This peak can be assigned to the reduction of the CuO phase to metallic copper in catalysts where there is a strong CuO-ZnO intermetallic interaction that increases the temperature range where copper reduction takes place (Wang et al., 2017). The CZAN-1 and CZAN-2 catalysts show a small reduction peak at temperatures around 285 °C followed by a large peak at about 350 °C. A study carried out by Shozi et al. (2017) on Cu-Re-ZnO catalysts concluded that these reduction peaks could indicate the reduction of CuO in two stages due to the influence of the support. The first stage of reduction of CuO to Cu_2O would happen at temperatures of 290 ºC and the second stage where Cu_2O would be reduced to metallic copper would occur around 340 ºC. According to Qi and Hu (2020), the ZnO phase could begin to reduce at temperatures around 450 ºC to 700 ºC, at which point it vaporizes and is lost, but this behavior has not been detected in the TPR profiles. Based on the TPR profiles, reduction temperatures were chosen for the complete reduction of copper, and the CZAN-1, CZAN-2, and CZAN-3 catalysts were activated at 375, 400, and 340 ºC respectively.

3.2 Catalytic activity

The reaction products were analyzed and the catalytic results of carbon yield to liquid and gaseous products are shown in Figure 3 (A) and the carbon selectivity to liquid products is shown in Figure 3 (B).

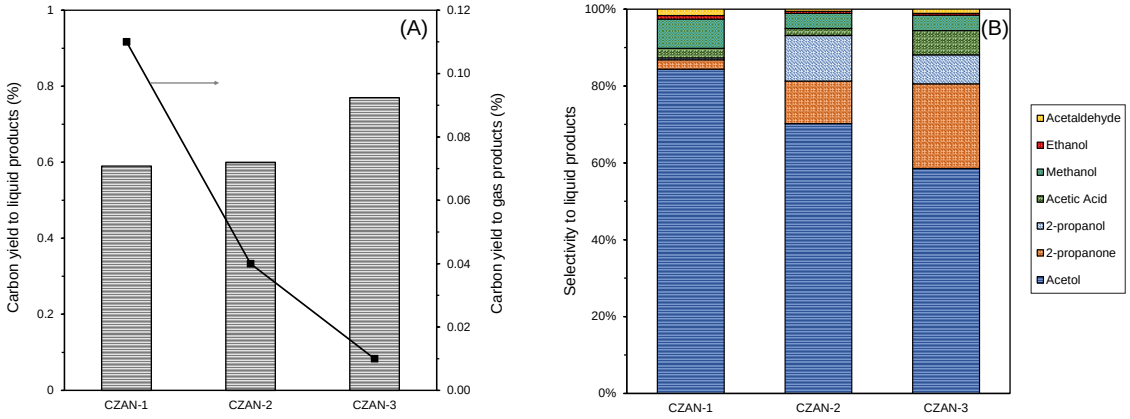

Figure 3: Carbon yield to liquid and gas products (A) and carbon selectivity to liquid products (B).

The gases produced during the reactions consist of H_2 and CO_2, and the carbon yield to gas products was minimal. The CZAN-1 catalyst exhibited the highest generation of carbon gases at 0.11 %, a performance that has subsequently decreased to 0.01 % with the CZAN-3 catalyst. In all experiments, the predominant gas has been H_2, with a volume percentage ranging between 82 and 84 %, and the residual component being CO_2.

Regarding the production of liquid compounds, the carbon yield to liquid products has exhibited a consistent pattern, registering at 0.6 % for both the CZAN-1 and CZAN-2 catalysts, and slightly elevated at 0.8 % for the CZAN-3 catalyst.
The primary liquid products quantified were acetol, 2-propanone, and 2-propanol. The dehydrogenation of 1,2-PDO to acetol has been the predominant route in all cases; however, clear differences can be discerned in the secondary products among the catalysts. The dehydration of 1,2-PDO to 2-propanone has occurred, with maximum reaction efficiency observed with the CZAN-3 catalyst, yielding a carbon selectivity to acetone of 22.1 %. Following closely is the CZAN-2 catalyst with 11.1 %, while the CZAN-1 catalyst exhibits a lower selectivity at 2.4 %. These results suggest that, despite achieving a relatively low carbon yield to liquid products, the catalysts demonstrate substantial selectivity towards 2-propanone. The third most generated compound in the CZAN-2 and CZAN-3 catalysts has been 2-propanol, with a carbon selectivity of 11.8 and 7.5 %, respectively. This indicates that a portion of the 2-propanone has undergone hydrogenation. In quantitative terms, the CZAN-3 catalyst has produced 1845 $\mu mol_{2\text{-propanone}}/mol_{1,2\text{-PDO}}$, the CZAN-2 catalyst 728 $\mu mol_{2\text{-propanone}}/mol_{1,2\text{-PDO}}$, and the CZAN-1 catalyst 154 $\mu mol_{2\text{-propanone}}/mol_{1,2\text{-PDO}}$. To ensure the significance of the catalysts' effects, the results were subjected to a one-way analysis of variance (ANOVA) with a 95 % confidence level. The analysis concluded that indeed the different catalysts have a statistically significant influence on the generation of 2-propanone ($p\text{-value}<0.05$).
The zinc content in the catalysts has thus directly impacted the yield of 2-propanone, with the CZAN-3 catalyst, featuring a lower proportion of zinc, demonstrating the highest selectivity. Furthermore, it has been observed that the CZAN-2 catalyst has been more active in the hydrogenation of 2-propanone to 2-propanol, leading to a reduction in 2-propanone selectivity. In comparison to the studied literature, the carbon selectivity to 2-propanone has been high despite achieving low conversions of 1,2-PDO. A study conducted by Sun et al. (2012), using a V_2O_5/Q_{10} catalyst with a 20 wt% aqueous 1,2-PDO solution at 250 ºC, yielded a 1,2-PDO conversion of 12.5 % and a selectivity to 2-propanone of 7.2 %, while the main product was propanal. This outcome indicates that under milder reaction conditions (227 ºC), a higher selectivity to 2-propanone has been achieved with the studied CZAN-3 catalyst.

4. Conclusions

The results demonstrated that the CZAN-3 catalyst is a mesoporous solid, whereas the CZAN-1 and CZAN-2 catalysts are macroporous or non-porous solids with lower specific surface areas. Sodium was incorporated during the coprecipitation stage, modifying the catalysts' properties. The metals were incorporated in the catalysts in the form of CuO, ZnO, and $NaAl_2O_4$. In the reaction, 1,2-PDO proved to be a highly unreactive compound with very low conversion. Under the studied reaction conditions gas production was minimal, and carbon conversion to liquid products was consistent across all three catalysts. The CZAN-3 catalyst exhibited the highest selectivity to 2-propanone (22.1 %) which could indicate that a lower zinc content favored the dehydration of 1,2-PDO to 2-propanone and could prevent the hydrogenation of 2-propanone to 2-propanol to a greater extent. The CZAN-3 catalyst was chosen as the most selective to 2-propanone and it generated the highest yield with 1845 $\mu mol_{2\text{-propanone}}/mol_{1,2\text{-PDO}}$. This catalyst showed the greatest S_{BET} and lowest sodium content. Experimental results have demonstrated that the dehydration of 1,2-PDO to 2-propanone is possible and further studies are required to optimize its production. This new method for the synthesis of 2-propanone would allow the generation of renewable biofuel for aviation by aldol condensation, reducing the carbon footprint of the sector.

Nomenclature

wt% – percentage by weight, %
S_{BET} – BET surface area, m^2/g
V_P – average pore volume, cm^3/g
d_p – average pore diameter, nm
X_{Gas} – carbon yield to gas products, %
X_{Liq} – carbon yield to liquid products, %
S_i – carbon selectivity to liquid product *i*, %
n_i – moles of product *i*, mol
n^0 – moles of carbon in 1,2-PDO fed, mol

Acknowledgments

The authors wish to express their gratitude to Project PID2020-114985RB-I00 funded by MCIN/AEI/10.13039/501100011033 and Aragón Government (Research Group Ref. T22_23R) for providing

frame support for this work. The authors would also like to acknowledge the use of the Servicio General de Apoyo a la Investigación – SAI, Universidad de Zaragoza. Alejandro Lete acknowledges the research grant from I3A.

References

Basu S., Sen A., 2021, A Review on Catalytic Dehydration of Glycerol to Acetol, Chembioeng Reviews, 8, 633-653.

Checa M., Nogales-Delgado S., Montes V., Encinar J., 2020, Recent Advances in Glycerol Catalytic Valorization: A Review, Catalysts, 10, 1279.

Courtney T. D., Nikolakis V., Mpourmpakis G., Chen J. G., Vlachos D. G., 2012, Liquid-phase dehydration of propylene glycol using solid-acid catalysts, Applied Catalysis A: General, 449, 59-68.

Inui, K., Kurabayashi, T., Sato, S., 2002, Direct synthesis of ethyl acetate from ethanol over Cu-Zn-Zr-Al-O catalyst, Applied Catalysis a-General, 237, 53-61.

Kinage A., Upare P., Kasinathan P., Hwang Y., Chang J., 2010, Selective conversion of glycerol to acetol over sodium-doped metal oxide catalysts, Catalysis Communications, 11, 620-623.

Kruissink E., Pelt H., Ross J., Vanreijen., 1981, The effect of sodium on the methanation activity of nickel-alumina coprecipitated catalysts, Applied Catalysis, 1, 23-29.

Li H. X., Edwards D. J., Hosseini M. R., Costin G. P., 2020, A review on renewable energy transition in Australia: An updated depiction, Journal of Cleaner Production, 242, 118475.

Mori K., Yamada Y., Sato S., 2009, Catalytic dehydration of 1,2-propanediol intro propanal, Applied Catalysis A: General, 366, 304-308.

Qi J., Hu X., 2020, The loss of ZnO as the support for metal catalysts by H-2 reduction, Physical Chemistry Chemical Physics, 22, 3953-3958.

Raso R., Lete A., García L., Ruiz J., Oliva M., Arauzo J., 2023, Aqueous phase hydrogenolysis of glycerol with in situ generated hydrogen over Ni/Al3Fe1 catalyst: effect of the calcination temperature, RSC Advances, 13, 5483-5495.

Restrepo J., Paternina-Arboleda C., Bula A., 2021, 1,2-Propanediol Production from Glycerol Derived from Biodiesel's Production: Technical and Economic Study, Energy, 14, 5081.

Shozi M., Dasireddy V., Singh S., Mohlala P., Morgan D., Iqbal S., Friedrich H., 2017, An investigation of Cu-Re-ZnO catalysts for the hydrogenolysis of glycerol under continuous flow conditions, Sustainable Energy & Fuels, 1, 1437-1445.

Song W., Zhu Q., Wang K., Zhu R., Ma Q., Zhao T., Guo Q., Gao X., Zhang J., 2023, Probing the Roles of Residual Sodium in Physicochemical Properties and Performance of FeAlNa Catalysts for Fischer-Tropsch Synthesis, Catalysts, 13, 1081.

Sun D., Yamada Y., Sato S., 2014, Production of propanal from 1,2-propanediol over silica-supported WO3 catalysts, Applied Catalysis A: General, 487, 234-241.

Wang W., Li X., Zhang Y., Zhang R., Ge H., Bi J., Tang M., 2017, Strong metal-support interactions between Ni and ZnO particles and their effect on the methanation performance of Ni/ZnO, Catalysis Science & Technology, 7, 4413-4421.

West R., Liu Z., Peter M., Gartner C., Dumesic J., 2008, Carbon-carbon bond formation for biomass-derived furfurals and ketones by aldol condensation in a biphasic system, Journal of Molecular Catalysis A: Chemical, 296,18-27

Yang Z., Qian K., Zhang X., Lei H., Xin C., Zhang Y., Qian M., Villota E., 2018, Process design and economics for the conversion of lignocellulosic biomass into jet fuel range cycloalkanes, Energy, 154, 289-297.